

ON THE INTERSECTION OF DIFFERENT SCATTERING PHASE FUNCTIONS IN THE UV REGION OF THE SPECTRUM

N.G. Ryabinina, Ya.A. Teifel', and V.E. Pavlov

*Academician V.G. Fesenkov Astrophysical Institute,
Academy of Sciences of the Kazakhstan SSR, Alma-Ata
Received May 10, 1989*

The displacement of the angle of intersection of the relative total luminance indicatrices with one another as well as with the spherical and Rayleigh luminance functions is studied with the help of model calculations of the luminance indicatrices of the daytime sky in the UV-region of the spectrum. The contribution of each term of the luminance indicatrix (aerosol, Rayleigh, and multiple scattering) to the drift of these intersection angles is determined. It is shown that in the UV-part of the spectrum multiple-scattering effects can cause the angles of intersection of the indicatrices to follow a loop-shaped trajectory.

INTRODUCTION

Phenomenological and statistical studies of the luminance of the clear daytime sky in different regions of the spectrum have also included a search for special points in the sky, in particular, the regions of the sky where the luminance does not depend on the form of the scattering phase function. This made it easier to model mathematically the scattering processes in the special regions and it has made it possible to find the correlations between an integral quantity – the light-scattering optical thickness of a dispersed medium τ –

$$\tau = 2\pi \int_0^{\pi} \mu(\varphi) \sin\varphi \, d\varphi \quad (1)$$

and the directional light-scattering coefficient $\mu(\varphi)$ for a definite scattering angle $\varphi = \varphi_0$, employed, for example, in the nephelometric method for determining τ . These questions, as a rule, are related, since the angle φ_0 is often chosen at the point of intersection of the real observed indicatrix

$$\mu_{\text{sp}}(\varphi_0 = \varphi_{\text{sp,ob}}),$$

where the relation

$$\tau_{\text{ob}} = 4\pi\mu_{\text{ob}}(\varphi_0) \quad (2)$$

holds. The quantity τ_{ob} is defined by the formula(1), in which the scattering phase function p is replaced by the luminance indicatrix μ_{ob} .

Experience has shown, however, that the position of the angles $\varphi_{\text{sp,ob}}$ and φ_0 , which at first appeared to be a constant for any scattering phase functions,¹⁻³

depends on the region of the spectrum where the measurements are performed, the layers of the atmosphere which are studied, and the optical states of the atmosphere.⁴⁻⁷

According to observations in the visible part of the spectrum the relative luminance indicatrices $f_{\text{ob}}(\varphi)$, equal to $\mu_{\text{ob}}\varphi/\tau_{\text{ob}}$, are practically equal to one another for scattering angles $\varphi \geq 40^\circ$ and intersect with the spherical indicatrix at $\varphi_{\text{sp,ob}} \sim 57^\circ$ (Refs. 1-3); the closest correlation between the integral τ_{ob} and the vector $\mu_{\text{ob}}(\varphi_0)$ was observed at the same angle $\varphi_0 = \varphi_{\text{sp,ob}} \sim 57^\circ$. In later works⁴⁻⁶ it was shown that the angle of intersection $\varphi_{\text{sp,ob}}$ of real luminance indicatrices and the spherical indicatrix as well as with $\mu_{\text{ob}}(\varphi_0)$ migrates insignificantly as a function of the zenith distance of the sun Z_\odot and the physical-geographical conditions of observation. For the surface layer, however, in the same spectral range $\varphi_0 \sim 45^\circ$ while $\varphi_{\text{sp,ob}} \sim 50 \div 55^\circ$.

The values of φ_0 and $\varphi_{\text{sp,ob}}$ in the near-IR region of the spectrum are the same.⁷ Our measurements of the sky luminance in the UV-region give completely different values: $\varphi_0 = \varphi_{\text{sp,ob}} \sim 60^\circ$ (Ref. 8).

It is natural to conjecture that this discrepancy in the values of φ_0 and $\varphi_{\text{sp,ob}}$ determined by the ratio of the single-scattering component $\mu_1 = \mu_a(\varphi) + \mu_R(\varphi)$ and the multiple-scattering component $\mu_2(\varphi)$ in the total luminance indicatrix

$$\mu_{\text{ob}}(\varphi) = \mu_1(\varphi) = \mu_1(\varphi) + \mu_2(\varphi)$$

as well as by the contribution of aerosol scattering $\mu_a(\varphi)$ and Rayleigh scattering $\mu_R(\varphi)$. In the surface layer of air the Rayleigh and multiple-scattering processes play a small role, and the scattering in this layer is mainly of an aerosol character. In the visible part of the spectrum the multiple-scattering effects

also are not determining. This suggests to us that the ultraviolet region of the spectrum is most favorable for studying changes in the position of the angle of intersection of different indicatrices both with one another (φ_i), with the spherical indicatrix ($\varphi_{sp,ob}$) and the Rayleigh indicatrix ($\varphi_{R,ob}$). Each component of the luminance indicatrix is manifested most clearly here.

In this paper the mechanism of migration of the angles φ_i , $\varphi_{sp,ob}$, and $\varphi_{R,ob}$ is studied in detail as a function of the contribution of different components of the total luminance. The computed and observed UV luminance indicatrices $f(\varphi)$ are analyzed. In these functions the Rayleigh component makes the largest contribution, the multiple-scattering component is significant, and under summer conditions reflected

light makes a small contribution to the sky luminance.⁸ For this reason the form of the observed indicatrices $f_{ob}(\varphi)$ is insensitive to variations of the aerosol, and it responds to the aerosol only near the sun. According to our experimental data, starting at scattering angles of the order of 25–30° and up to $\varphi \sim 160^\circ$, the relative luminance indicatrices $f_{ob}(\varphi)$ are identical, and their form remains the same at different geographical points (Fig. 1).⁸ The sky luminance in the halo part is determined primarily by scattering by large aerosol particles and is approximated well by calculations based on the Young aerosol scattering functions with the particle-size distribution parameter $\nu^* \sim 2.5$, the upper limit of the particle radius $r_{max} \sim 5\text{--}10 \mu\text{m}$, and the real refractive index $n = 1.5$ (Refs. 9–12).

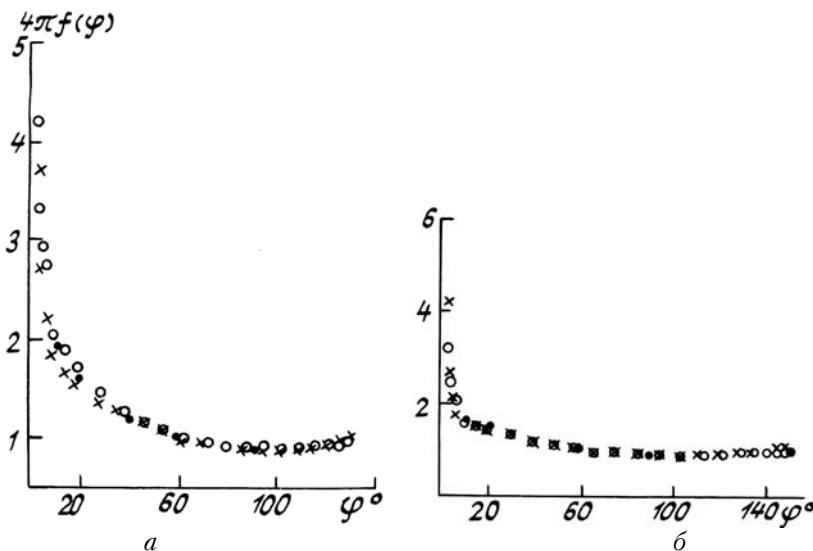


FIG. 1. The relative luminance indicatrices obtained from observations:

a) $Z_{\odot} \sim 64^\circ$; dots — Assy Plateau, August 17, 1976, (a.m.), $\tau_a = 0.11$; $\lambda = 313.5 \text{ nm}$, ($Z_{\odot} = 64.15^\circ$); circles — Kryzhanovka, September 6, 1972, (a.m.), $\tau_a = 0.75$; $\lambda = 311 \text{ nm}$, ($Z_{\odot} = 64.1^\circ$); crosses — Kirbaltabai, September 18, 1973, (p.m.), $\tau_a = 0.34$; $\lambda = 311 \text{ nm}$, ($Z_{\odot} = 63.6^\circ$);
b) $Z_{\odot} \sim 72\text{--}73^\circ$; dots — Assy Plateau, August 20, 1976, (p.m.), $\tau_a = 0.09$; $\lambda = 313.5 \text{ nm}$, ($Z_{\odot} = 72.3^\circ$); circles — Kryzhanovka, September 8, 1972, p.m., $\tau_a = 0.38$; $\lambda = 311 \text{ nm}$, ($Z_{\odot} = 72.7^\circ$); crosses — Kirbaltabai, September 17, 1973, (p.m.), $\tau_a = 0.27$; $\lambda = 311 \text{ nm}$, ($Z_{\odot} = 71.9^\circ$).

The observed UV luminance indicatrices $f_{ob}(\varphi)$, as we have established in Refs. 8–11, intersect with the spherical indicatrix $f_{sp}(\varphi)$ near the scattering angle $\varphi_{sp,ob} \sim 60^\circ$. Additional studies¹⁴ have shown that the location of $\varphi_{sp,ob}$ is related with the turbidity of the atmosphere, characterized by the aerosol optical thickness τ_a . For example, for the settlement of Kryzhanovka in the Odessa region, where the aerosol optical thickness, averaged over a season of observations, for the wavelength $\lambda \sim 337 \text{ nm}$ $\bar{\tau}_a \sim 0.6$, $\varphi_{sp,ob} \sim 57\text{--}59^\circ$; for the settlement of Kirbaltabai and at the Astrophysical Institute of the Academy of Sciences of the Kazakhstan SSR, where

$\bar{\tau}_a \sim 0.25$, ($\bar{\varphi}_a \sim 0.24$); and, for the high-mountain Assy-Turgen Plateau, where $\bar{\tau}_a \sim 0.08$, $\varphi_{sp,ob} \sim 55^\circ$.

We analyzed the intersection of different indicatrices in the UV region of the spectrum with the help of model Monte-Carlo calculations of the scattering phase function $\mu_{ob}(\varphi)$, performed at the Computer Center of the Siberian Branch of the Academy of Sciences of the USSR¹⁵ based on the Young aerosol indicatrices $\mu_a(\varphi)$ with the particle-size distribution parameters $\nu^* = 2$ and 4; this made it possible to place the real values of the indicatrices between the computed values. By varying the aerosol optical thickness τ_a over the range 0.15–0.70, the Rayleigh optical thickness τ_R

over the range 0.415–1.110, and the ozone absorption thickness τ_{oz} over the range 0.01–1.110 it was possible to cover the wavelength range 373–307 nm under different physical-geographical conditions. The summer albedo α of the underlying surface is equal to 0.045 (Ref. 8). The zenith distances of the sun were set equal to $Z_{\odot} = 63, 72, \text{ and } 76^{\circ}$, which ensured that multiple-scattering effects make a different contribution to the luminance distribution along the sun's parallel of altitude.

The problem was to determine the effect of each component $\mu_a(\varphi), \mu_R(\varphi)$, and $\mu_2(\varphi)$ of the indicatrix $\mu_{ob}(\varphi)$ on the position of the point of intersection of the luminance indicatrices with one another and with the spherical and Rayleigh functions, and ultimately to prove the empirical fact that near the angles $\varphi \sim 55\text{--}60^{\circ}$ the sky luminance in the UV region of the spectrum is independent of the form of the scattering phase function.

The investigations were organized as follows. The Young indicatrices were studied first and the Rayleigh indicatrices, followed by the multiple-scattering components, were added to them. Next the displacement of the point of 'intersection' of the indicatrices owing to one or another term was traced. We employed this method in Refs. 14 and 16.

INTERSECTION OF THE MODEL INDICATRICES IN THE UV REGION OF THE SPECTRUM WITH ONE ANOTHER

The Young aerosol indicatrices $f_a(\varphi) = \mu_a(\varphi)/\tau_a$, employed in the calculations, with $v^* = 2$ and 4 intersect in the forward hemisphere at $\varphi_i \sim 18^{\circ}$. Rayleigh scattering shifts the angles φ_i , into the region 22–26°. The indicatrices for the first scattering $f_1(\varphi) = \mu_a(\varphi) + \mu_R(\varphi)/(\tau_a + \tau_R)$ distinguished by the Young parameter ($v^* = 2$ and 4), intersect precisely here for all cases modeled when the ratio of the aerosol and Rayleigh optical thicknesses τ_a/τ_R falls into the range 0.135–1.687.

The multiple-scattering contribution $\mu_2(\varphi)$ shifts φ_i toward larger angles, so that the computed values

$$f_{ob}(\varphi) = \mu_a(\varphi) + \mu_R(\varphi) + \mu_2(\varphi)/\tau_{ob},$$

based on the Young functions with $v^* = 2$ and 4 for these cases, intersect with one another already at $\varphi_i = 25\text{--}50^{\circ}$, when the sun's zenith distance $Z_{\odot} \sim 63^{\circ}$. In addition, the angle φ_i is all the larger the larger the value of τ_a . However for total scattering thicknesses $\tau_a + \tau_R > 1.5$ and $Z_{\odot} > 75^{\circ}$ the angle of intersection φ_i traverses a loop and shifts in the opposite direction — toward 30–8°. Under these conditions the multiple-scattering effects are determining, the multiple-scattering indicatrices become virtually spherical, and the total functions $\mu_{ob}(\varphi)$ for $v^* = 2$ and 4 lose their asymmetry and converge closer to one another not only at middle but also at small scattering angles, so that φ_i starts to decrease.

The drift of the angle φ_i along a loop-shaped trajectory, owing to the increase in the contribution of the higher orders of scattering to $\mu_{ob}(\varphi)$, makes it possible to explain the statistical average value $\varphi_i \sim 25\text{--}30^{\circ}$ for all observed luminance indicatrices in the UV region. In the visible section of the spectrum, however, the scattering thicknesses τ_1 are, as a rule, not large enough for the multiple-scattering effects to cause a return to small angles. Apparently, this is why the average statistical value of the angle φ_i is equal to $\sim 40^{\circ}$ (Ref. 3).

Comparison of the observed luminance indicatrix¹⁴ and the Monte-Carlo luminance indicatrices showed that in the UV region of the spectrum the observed absolute luminance indicatrices $\mu_{ob}(\varphi)$ fall between the computed indicatrices; the computed indicatrices $\mu_{ob}(\varphi)$, differing only by the value of the size distribution parameter of the aerosols ($2 \leq v^* \leq 4$) in the region of scattering angles $\varphi_i \leq \varphi < 160^{\circ}$, are identical to within the limits of error in the calculation of $\mu_{ob}(\varphi)$, which are set equal to the errors in the experimental determination of $\mu_{ob}(\varphi)$. This is why in the spectral region under study it makes sense to talk about not the points of intersection of the observed relative indicatrices with one another but rather about the neighborhood of scattering angles in the forward hemisphere near φ_i where the observed f_{ob} (or model) indicatrices start to separate owing to the difference in the aerosol components.

INTERSECTION OF THE MODEL FIRST-SCATTERING INDICATRICES WITH SPHERICAL AND RAYLEIGH INDICATRICES

To find the region of scattering angles where the sky luminance in the UV region of the spectrum does not depend on the form of the indicatrix the points of intersection of the model indicatrices $f_{ob}(\varphi)$, based on the Young indicatrices $f_a(\varphi)$ for $v^* = 2$ and 4, with the spherical and Rayleigh indicatrices were determined. These points should obviously be located at angles $\varphi < \varphi_i$.

It was established first that the Young first-scattering indicatrices intersect with the spherical and Rayleigh indicatrices at the angles $\varphi_{sp,a}$ and $\varphi_{R,a}$, presented in Table 1.

TABLE 1.

The scattering angles φ at which the model Young indicatrices ($v^ = 2$ and 4) intersect with the spherical and Rayleigh indicatrices.*

v^*	φ	
	$\varphi_{sp,a}^0$	$\varphi_{R,a}^0$
2	51	49
4	60.5	63.5

Adding the Rayleigh component $\mu_R(\varphi)$ to $\mu_a(\varphi)$ shifts the point of intersection $\varphi_{sp,1}$ of the total first-scattering indicatrix $f_1(\varphi)$ with the spherical function $f_{sp}(\varphi)$.

Figure 2 shows the displacement of $\varphi_{sp,1}$ as a function of the asymmetry Γ_1 of the scattering phase functions:

$$\Gamma_1 = \int_0^{\pi/2} \mu_1(\varphi) \sin\varphi \, d\varphi / \int_0^{\pi/2} \mu_a(\varphi) \sin\varphi \, d\varphi.$$

Γ_1 varies in accordance with the relative contributions of μ_a and μ_R to μ_1 in the range from $\Gamma_a = 1$. Figure 2 shows that as Rayleigh scattering becomes more important the values of $\varphi_{sp,1}$ approach from $\varphi_{sp,a}$ ($v^* = 2$ and 4), giving two branches of points (Table I), $\varphi_{sp,R} = 54.7^\circ$ as in the case of a purely Rayleigh indicatrix. For the model indicatrices which we analyzed the angle $\varphi_{1,sp}$ is equal to $51-53^\circ$ ($v^* = 2$) and $54.7-59^\circ$ ($v^* = 4$).

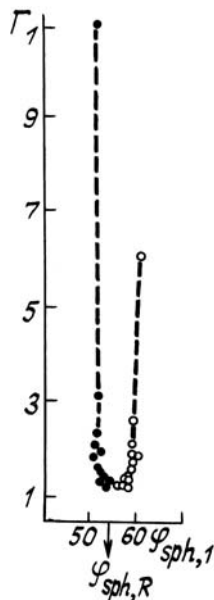


FIG. 2. The displacement of the point of intersection $\varphi_{sp,1}$ of the first-scattering indicatrices with the spherical indicatrix with a change in asymmetry: $v^* = 2$ (dark circles) and $v^* = 4$ (light circles).

As regards the intersection of model first-scattering indicatrices $f_1(\varphi)$ with the Rayleigh indicatrix $f_R(\varphi)$, the angle $\varphi_{1,R}$ falls into the range $46-52^\circ$ for $v^* = 2$ and $60-63^\circ$ for $v^* = 4$, i.e., it is determined primarily by the intersection of $f_a(\varphi)$ with $f_R(\varphi)$ (Table I). Figure 3 shows $\varphi_{1,R}$ as a function of Γ_1 .

EFFECT OF MULTIPLE SCATTERING ON THE INTERSECTION OF DIFFERENT INDICATRICES

The addition of $\mu_2(\varphi)$, determined by the multiple scattering of light, to the asymmetric model

first-scattering indicatrices $\mu_1(\varphi)$ shifts the point of intersection $\varphi_{sp,ob}$ of the indicatrices $f_{ob}(\varphi)$ with the spherical indicatrix into the region of angles larger than $\varphi_{sp,1}$ (Fig. 4a, b, c, d). This shift is all the larger the larger the value of τ_a , but as Z_\odot changes it can acquire a loop-shaped character, if $\tau_R > \tau_a$ or $\tau_R > 1$ (Figs. 4c and d). All cases covered by the model calculations¹⁴ give the intervals $52-75^\circ$ ($v^* = 2$) and $58-75^\circ$ ($v^* = 4$) for $\varphi_{sp,ob}$.

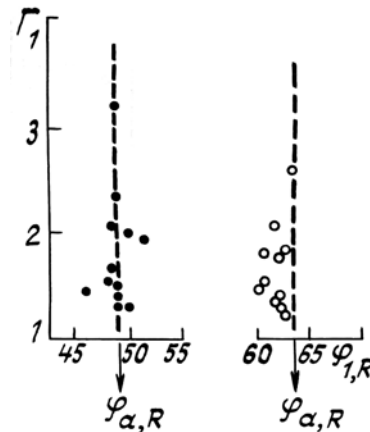


FIG. 3. The position of the point of intersection $\varphi_{R,1}$ of the first-scattering indicatrices with the Rayleigh indicatrix as a function of the asymmetry of the model indicatrices $v^* = 2$ (dark circles) and $v^* = 4$ (light circles).

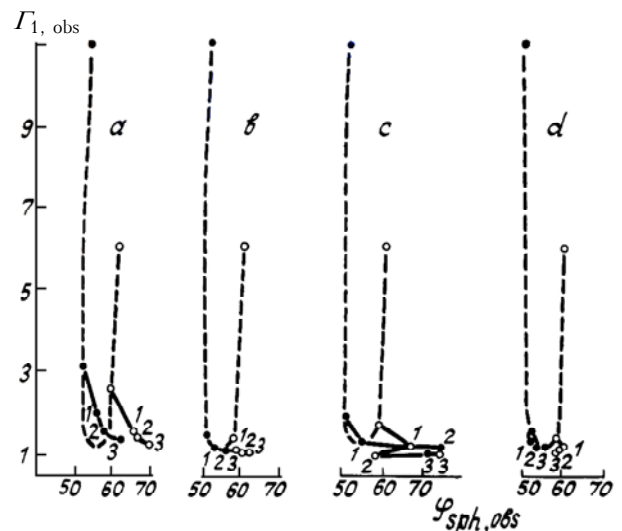


FIG. 4. Drift of the point of intersection $\varphi_{sp,ob}$ of the model indicatrices $f_{ob}(\varphi)$ with the spherical indicatrix accompanying a change of asymmetry Γ_{ob} . 1 - $Z_\odot = 63^\circ$, 2 - $Z_\odot = 72^\circ$, 3 - $Z_\odot = 76^\circ$; dark circles - $v^* = 2$; light circles - $v^* = 4$, a) $\tau_a = 0.70$, $\tau_R = 0.415$, $\lambda = 373$ nm; b) $\tau_a = 0.30$, $\tau_R = 0.975$, $\lambda = 311$ nm; c) $\tau_a = 0.70$, $\tau_R = 1.11$, $\lambda = 306,8$ nm; d) $\tau_a = 0.15$, $\tau_R = 0.415$, $\lambda = 373$ nm.

Table II also illustrates the fact that multiple scattering increases $\varphi_{sp,ob}$ for asymmetric indicatrices. The table gives the values of $\varphi_{sp,ob}$ for two elongated indicatrices $\mu_{ob}(\varphi)$ VII and VIII according to the data from Ref. 17.

TABLE II.

The position of the angle of intersection of the indicatrices $f_{ob}(\varphi)$ (VII and VIII, Ref. 17) and the Rayleigh indicatrix (Ref. 18) with the spherical indicatrix accompanying a change in the contribution of multiple scattering.

indica- trix	τ_1	f_1		$Z_\odot = 60^\circ$		$Z_\odot = 75^\circ$	
		$\varphi_{sp,1}^0$	$\varphi_{R,1}^0$	$\varphi_{sp,2}^0$	$\varphi_{sp,ob}^0$	$\varphi_{sp,2}^0$	$\varphi_{sp,ob}^0$
VII	0.6	57.6	58.5	72	60	72	62
	0.8			73	61	73.7	64.7
VIII	0.6	54.8	54.5	67	59	67.5	60
	0.8			68.5	60	69.5	62.2
f_R	0.4	54.7	indi- catrici- ces are iden- tical at all points	55	54.7	50	53
	0.6			56.5	55	53.5	54.7
	0.8			56	55	52.5	53.5

Continuing the analysis of Table II we note the following. In the case of scattering by molecules at

middle and large angles φ the multiple-scattering component is substantially spherical¹⁸ and for this reason it does not change $\varphi_{sp,R(ob)}$ right up to $Z_\odot \sim 75^\circ$. When the sun's zenith distances reach $Z_\odot \geq 75^\circ$ the total indicatrix $\mu_{R(ob)} = \mu_R + \mu_{2R}$ approaches a spherical function, and $\varphi_{sp,R(ob)}$ shifts toward smaller angles: $\varphi_{sp,R(ob)} < \varphi_{sp,R}$. The last result is also true for the total indicatrices $(\mu_R + \mu_{2R})$ in the UV region of the spectrum, when $\mu_2 (Z_\odot > 80^\circ)$ becomes the dominant component and the asymmetry Γ_{ob} approaches unity, but does not reach it (the deep regime)³.

Since multiple scattering causes the indicatrix $(\mu_R + \mu_{2R})$ to approach a spherical form the conditions for intersection of the observed indicatrices μ_{ob}/τ_{ob} with $(\mu_R + \mu_{2R})/\tau_{ob}$ are close to the conditions for intersection of μ_{ob}/τ_{ob} with the spherical indicatrix: $\varphi_{sp,ob} \approx \varphi_{R(ob),ob}$.

Thus the use of computed model indicatrices μ_{ob} based on the Young indicatrices with $v^* = 2$ and 4 for the UV region of the spectrum, when the scattering thicknesses fall in the range $0.4 \leq \tau_R \leq 1.11$ and $0.15 \leq \tau_a \leq 0.7$, covering the indicatrices μ_{ob} which we actually observed, as well as the asymmetric phase functions VII and VIII (for anisotropic scattering and thicknesses $\tau_1 = 0.6$ and 0.8), modelled at the Institute of Atmospheric Physics of the Academy of Sciences of the USSR,¹⁷ showed that in the case when the scattering thicknesses τ_1 are equal and the sun's zenith distances Z_\odot fall into the range $\sim 63-75^\circ$ the point of intersection of the model indicatrices μ_{ob}/τ_{ob} with the spherical and Rayleigh indicatrices can drift over a quite wide range of scattering angles $\Delta\varphi_{ob(sp,R(ob))} = 52 \div 75^\circ$.

TABLE III.

The correlation R between $\mu_{ob}(60^\circ)$ and τ_{ob} and the coefficient of proportionality $\gamma(60^\circ)$ between these quantities in the UV absorption band of ozone, $\lambda < 340$ nm.

location of observation	$\mu_{ob}(60^\circ)$	$\sigma\mu_{ob}(60^\circ)$	τ_{ob}	$\sigma\tau_{ob}$	$R\mu_{ob}\tau_{ob}(60^\circ)$	$\gamma(60^\circ)$	$\sigma\tau(60^\circ)$
Assy Plateau ↓ 1976 $N_{sl} = 16$	0.15	0.02	2.01	0.21	0.97	13.0	0.4
Astrophysics Academy of Sciences of Kazakhstan SSR ↓ 1971 $N = 162$	0.38	0.18	4.86	2.25	1.00	12.9	0.4
Kirbaltaba ^y ↓ 1973 $N = 43$	0.85	0.80	10.9	10.1	1.00	12.7	0.2
Kryzhanovka ↓ 1972 $N = 51$	2.43	2.74	30.6	34.3	1.00	12.6	0.2
All locations of observation						12.8	0.3

N^* is the number of cases analyzed.

According to our data, however, the real indicatrices μ_{ob} in the UV region of the spectrum exhibit a significantly smaller range of forms than the computed indicatrices analyzed here and, as we mentioned, they are close to the model luminance indicatrices based on the Young aerosol indicatrices with the distribution parameter $\nu^* \sim 2.5$. As a result, when the zenith distance of the sun's parallel of altitude is limited to $Z_{\odot} < 75^\circ$ (where μ_{ob} were measured) the interval $\Delta\varphi_{ob(sp,R(ob))}$ becomes narrower: $\sim 55\text{--}65^\circ$. This is why the average statistical value of the coefficient of proportionality $\gamma(60^\circ)$ between $\mu_{ob}(60^\circ)$ and τ_{ob} is close to 4π , as in the case of the spherical indicatrix,

$$\tau_{ob} = \gamma(60^\circ) \mu_{ob}(60^\circ).$$

This is illustrated in Table III, where the values of $\gamma(60^\circ)$ for the internal of the sun's zenith distances indicated above are presented for four locations of observations.

Analysis of Table III shows that the value of $\overline{\gamma(60^\circ)}$ ranges from 12.6 ($\sim 4\pi$) for Kryzhanovka near Odessa, where the indicatrix μ_{ob} is substantially of an aerosol character, up to 13 at the high-mountain plateau of Assy, when the observed indicatrices are practically of the Rayleigh form and intersect with the spherical indicatrix at $\varphi_i \sim 55^\circ$ and not at 60° . Another important conclusion that can be drawn from Table III and everything else said above is that in spite of the significant spread in $\sigma\mu_{ob}(60^\circ)$ and $\sigma\tau_{ob}$, the absolute values of the directional light-scattering coefficient $\mu_{ob}(60^\circ)$, and the integral τ_{ob} , obtained using a formula analogous to (1), in the UV region of the spectrum for different geographical points relative values $\mu_{ob}(60^\circ)/\tau_{ob}$ are practically identical not only at different locations of observations, but they differ little from $\mu_{sp}(60^\circ)/\tau_{ob}$ for the spherical luminance indicatrix and $\mu_R(60^\circ)/\tau_{ob}$ for the Rayleigh luminance indicatrix. This indicates that near $\varphi_i \sim 60$ the sky luminance in the UV region of the spectrum does not depend on the form of the indicatrix: here the real indicatrices intersect the spherical and Rayleigh indicatrices.

CONCLUSIONS

1. Owing to the overall approach employed from the spectral viewpoint the results obtained in this work based on model calculations in the UV region of the spectrum are generally valid: the Rayleigh and multiple-scattering phase functions are added to the Young (naturally averaged) phase functions.

2. It was found that changing the ratio of the aerosol, Rayleigh, and multiple-scattering components, whose absolute contribution to the luminance indicatrix is determined by the optical thicknesses ($\tau_a = 0.15\text{--}0.7$ and $\tau_R = 0.45\text{--}1.11$) and the sun's zenith distance ($Z_{\odot} = 63\text{--}76^\circ$), results in a

shift of the position of the angle of intersection $\varphi_{ob,sp(R)}$ of the computed indicatrices with the spherical indicatrix in the range $51\text{--}75^\circ$ ($\nu^* = 4$) and with the Rayleigh indicatrix in the range $46\text{--}75^\circ$ ($\nu^* = 2$) and $60\text{--}75^\circ$ ($\nu^* = 4$), including also the first-scattering indicatrix. It was established that in the UV region of the spectrum the multiple-scattering effects can cause this angle to drift over a loop-shaped trajectory. As a rule, for the luminance indicatrix in which Rayleigh scattering does not predominate multiple-scattering corrections increase, as compared with the first-scattering indicatrices, the angle $\varphi_{sp,ob}$ of intersection of the total indicatrices with the spherical indicatrix. However when $\tau_R > \tau_a$ or $\tau_R > 1$ the angle $\varphi_{sp,ob}$ at first increases as Z_{\odot} increases, but at zenith distances $Z_{\odot} > 76^\circ$ it starts to move in the opposite direction — toward smaller angles. The behavior of the angle of intersection φ_i of the luminance indicatrices μ_{ob}/τ_{ob} for $\nu^* = 2$ and 4 with one another is analogous; φ_i ranges from 8° to 50° .

3. The variability of the observed indicatrices f_{ob} and the optical aerosol thicknesses τ_a at a specific location is much narrower than in the case of the modeled indicatrices. In the UV region of the spectrum the form of the observed indicatrices is described well by the model Young indicatrix with the particle-size distribution parameter $\nu^* \sim 2.5$. For this reason the relative observed indicatrices μ_{ob}/τ_{ob} are virtually identical at scattering angles $\varphi > \varphi_i$ irrespective of the meteorological and geographical conditions of the measurements of the sky luminance, and they become separated only for $\varphi < \varphi_i$. The angle of intersection φ_i of the observed indicatrices with one another falls into a narrow range: $25\text{--}30^\circ$.

4. Since variations of the aerosol are manifested in the UV region of the spectrum only in the halo part of the observed indicatrices, which makes an insignificant contribution to the observed indicatrices, which makes an insignificant contribution to the integral τ_{ob} , the value of the integral τ_{ob} does not depend on the form of the scattering phase function; the relative observed luminance indicatrices f_{ob} intersect with the spherical and Rayleigh indicatrices in the range of angles $\varphi_{ob,(sp,R)} = 55\text{--}60^\circ$; the luminance of the sky near these angles does not depend on the form of the scattering phase function, so that the nephelometric relation, relating the integral τ_{ob} with the directional light-scattering vector μ_{ob} , has the same form (2) as for the spherical indicatrix.

REFERENCES

1. E.V. Pyaskovskaya-Fesenkova, *Investigation of Light Scattering in the Earth Atmosphere* (Izd. Akad. Nauk SSSR, Moscow, 1957).
2. V.E. Pavlov, *Astron. Zh.*, No. 43, 889 (1966).
3. G.Sh. Livshitz, *Light Scattering in the Atmosphere* (Nauka, Alma-Ata, 1965).

4. O.D. Barteneva, E.I. Dovgyallo, and E.A. Polyakova, Tr. Gl. Geofiz. Obs., No. 220, 101 (Gidrometeoizdat, Leningrad, 1967).
5. V.I. Kushpil, L.F. Petrova and K.F. Khazak, *Light Scattering in the Earth's Atmosphere* (Nauka, Alma-Ata, 1972).
6. S.I. Avdyushin, E.E. Artyomkin, V.N. Emel'yanov, A.E. Mikirov, and B.I. Semengin, Atmospheric Optics, Proceedings of the Institute of Applied Geophysics No. 32, 3 (Gidrometeoizdat, Moscow, 1977).
7. A.I. Ivanov, G.Sh. Livshitz, and I.A. Fedulin, *Scattering of IR Radiation in the Cloudless Atmosphere*, (Nauka, Alma-Ata, 1974).
8. V.E. Pavlov, N.G. Ryabinina, and Ya.A. Teifel', et al., *The Scattered Radiation Field in the Earth's Atmosphere* (Nauka, Alma-Ata, 1974).
9. N.G. Ryabinina, *Atmospheric Transmission and the Daytime Sky Luminance in the Ozone Absorption Band*, Author's Abstract of the Candidates Dissertation in Physical-Mathematical Sciences, Tomsk State University, Tomsk (1982).
10. Ya.A. Teifel in: *Abstracts of Reports at the All Union Conference on Atmospheric Optics*, Part 2, 24, Tomsk (1976).
11. N.G. Ryabinina, *Abstracts of Reports at the All-Union Conference on Propagation of Optical Radiation in Dispersive Media* (Gidrometeoizdat, Moscow, 1978).
12. Ya.A. Teifel, *Light Scattering in the Earth's Atmosphere* (Nauka, Alma-Ata, 1980).
13. L.A. Egorova, V.E. Pavlov, N.G. Ryabinina, et al., *Extinction of Light in the Earth's Atmosphere* (Nauka, Alma-Ata, 1976).
14. N.G. Ryabinina and Ya.A. Teifel, *Abstracts of Reports at the Second All-Union Conference on Laser Propagation in Dispersive Media*, Part 1, 88, Obninsk (1982).
15. M.A. Nazaraliev, V.E. Pavlov, and N.G. Ryabinina, *Studies of the Optical Characteristics of the Atmosphere in the Shortwave Spectrum* (Nauka, Alma-Ata, 1981).
16. N.G. Ryabinina, Ya.A. Teifel, *Proceedings of the Third All-Union Conference on Atmospheric Optics and Actinometry*, Tomsk Affiliate of the Siberian Branch of the USSR Academy of Sciences, Part 1, 320, Tomsk (1983).
17. E.M. Feigelson, M.S. Malkevich, S.Ya. Kogan, et al., *Calculations of the Luminance in the Atmosphere with Anisotropic Scattering*, (Izd. Akad. Nauk SSSR, Moscow, 1957).
18. K.L. Coulson, J.V. Dave, Z. Sekera, *Tables Related to Radiation Emerging from a planetary Atmosphere with Rayleigh Scattering*, Univers, of California Press. Berkeley. Los Angeles, p. 548 (1960).